SPHALERONS, DEFORMED SPHALERONS AND NORMAL MODES

Y. BRIHAYE

Faculté des Sciences, Université de Mons-Hainaut
B-7000 Mons, Belgium

J. KUNZ

Instituut voor Theoretische Fysica, Rijkuniversiteit Utrecht
NL-3508, The Netherlands
and
FB Physik, Postfach 2503, Universität Oldenburg
Germany

(Received January 27, 1992)

Topological arguments suggest that the Weinberg-Salam model possesses unstable solutions, sphalerons, representing the top of energy barriers between inequivalent vacua of the gauge theory. In the limit of vanishing Weinberg angle, such unstable solutions are known: the sphaleron of Klinkhamer and Manton and at large values of the Higgs mass in addition the deformed sphalerons. Here a systematic study of the discrete normal modes about these sphalerons for the full range of the Higgs mass is presented. The emergence of deformed sphalerons at critical values of the Higgs mass is seen to be related to the crossing of zero of the eigenvalue of the particular normal modes about the sphaleron.

PACS numbers: 11.15.Kc, 11.90.+t

1. Introduction

The standard model of electroweak interactions does not strictly conserve baryon and lepton number [1]. The suggestion that the rate of baryon number violation is unsuppressed at high temperature [2] has motivated a lot of effort to estimate the rate of baryon number changing processes, which occur only through transitions between topologically distinct vacua of the theory [1,3]. In the high temperature regime (just below the electroweak phase transition $T \approx 100 - 350$ GeV) they are mediated by sphalerons [4],

static unstable solutions of the equations of motion, which represent the top of energy barriers between inequivalent vacua.

Classical configurations corresponding to the minimal energy barrier between topologically inequivalent vacua constitute physically relevant objects of the theory. Since the equations of motion are non-linear, finding solutions represents a non-trivial exercise. The construction of solutions can be simplified by imposing particular symmetries. In the present case one usually considers the limit of vanishing Weinberg angle θ_W, which then allows for a generalized spherically symmetric ansatz for the fields. (One assumes, that this is a good approximation for the relevant solution of the full theory.) The sphaleron of Klinkhamer and Manton [4] (in fact discovered earlier [5]) was identified as such configuration. Recently new classical solutions [6-8] of the equations of motion were shown to exist for sufficiently high values of the Higgs mass (for $M_H > 12M_W$). The energy of these new "deformed sphalerons" is lower than the one of sphaleron of Klinkhamer and Manton. When existing, the lowest of the new solutions constitutes the minimal energy barrier between distinct vacua [9].

Once the sphaleron is identified, the rate of baryon number changing transitions can be computed by using the techniques of non-equilibrium statistical mechanics [10,11]. The key ingredient is the computation of the determinant of small fluctuations around the minimal energy barrier configuration [12]. The computation of this determinant represents a formidable task. The problem was first addressed by using various approximation techniques [12-14], recently Carson *et al.* [15] presented an exact numerical calculation for the interval $0.1 \leq M_H/M_W \leq 4.5$ of the Higgs mass. These authors exploit the symmetries of the sphaleron, identify its SU(2) stability group and the corresponding generators, say $\boldsymbol{J}$; then they decompose the fluctuations in the basis of the spherical harmonics associated with $\boldsymbol{J}$ and finally compute the determinant.

The negative normal modes and the zero modes needs special consideration in the evaluation of the transition rate. The objective of this paper is to report a systematic study of the discrete normal modes about sphalerons and deformed sphalerons for a spherically symmetric ansatz for the fluctuations, where we consider the full range of the Higgs mass, *i.e.* $0 \leq M_H \leq \infty$. The subspace of spherically symmetric configurations corresponds to the lowest quantum number of the operator $\boldsymbol{J}$. All directions of instability of the sphalerons and of the deformed sphalerons have so far been identified in this particular channel [8,13,16,17].

In Section 2 we describe the model, the ansatz and we revisit the main features of the sphalerons and deformed sphalerons. In Section 3 we establish the eigenvalue equations to be solved in the analysis of the normal modes. The numerical results for these modes, such as the number of dis-

crete modes and the signs of their eigenvalues, are discussed in Section 4. The conclusions are drawn in Section 5.

2. Classical equations

The lagrangian density of the SU(2)-Higgs model reads

$$L = -\frac{1}{2g^2}\,\mathrm{Tr}(F^{\mu\nu}F_{\mu\nu}) + (D_\mu\phi)^\dagger(D^\mu\phi) - \lambda\Big(\phi^\dagger\phi - \frac{v^2}{2}\Big)^2 \tag{2.1}$$

with the standard definitions for the covariant derivative and gauge field strengths

$$F_{\mu\nu} = \partial_\mu V_\nu - \partial_\nu V_\mu - i[V_\mu, V_\nu], \tag{2.2}$$

$$D_\mu\phi = (\partial_\mu - iV_\mu)\phi. \tag{2.3}$$

The gauge symmetry is spontaneously broken *via* the Higgs potential, leading to a non-vanishing expectation value for the Higgs field

$$\langle\phi\rangle = \frac{v}{\sqrt{2}}\begin{pmatrix}0\\1\end{pmatrix} \tag{2.4}$$

and giving masses to the gauge and Higgs bosons:

$$M_{\mathrm{W}} = \frac{vg}{2}, \qquad M_{\mathrm{H}} = v\sqrt{2\lambda}. \tag{2.5}$$

In the following, we choose the vector boson mass $M_{\mathrm{W}} = 83$ GeV and the coupling constant $g = 0.67$.

The classical configurations considered here are static and spherically symmetric, *i.e.* we restrict the fields to the following forms

$$\phi(x) = \frac{v}{\sqrt{2}}\big(H + iK(\hat{x}\cdot\vec{\tau})\big)\begin{pmatrix}0\\1\end{pmatrix}, \tag{2.6a}$$

$$V_0 = 0, \quad V_k = \frac{1}{2r}\Big((1-f_A)T_k^{(1)} + f_B T_k^{(2)} + f_C T_k^{(3)}\Big) \tag{2.6b}$$

with the tensors T_i

$$T_i^{(1)} = \varepsilon_{ijk}\hat{x}_j\tau_k, \quad T_i^{(2)} = (\delta_{ij} - \hat{x}_i\hat{x}_j)\tau_j, \quad T_i^{(3)} = \hat{x}_i\hat{x}_j\tau_j, \tag{2.7}$$

where f_A, f_B, f_C, H and K are functions of the radial variable r. Under the parity operator, the functions f_A and H remain invariant while f_B, f_C and K change sign.

In order to identify the stability group of the configurations assuming the form (2.6), one considers SO(4) transformations, which in the fundamental representation act on the 4-vector $(-\mathrm{Re}\,\phi_1, \mathrm{Im}\,\phi_1, \mathrm{Re}\,\phi_2, \mathrm{Im}\,\phi_2)$. It follows (see Ref. [15], whose notations we use) that fields of the form (2.6) are invariant under the SU(2) symmetry group generated by $\boldsymbol{J}$ with

$$\boldsymbol{J} = \boldsymbol{L} + \boldsymbol{S} + \boldsymbol{I} + \boldsymbol{K}, \tag{2.8}$$

where $\boldsymbol{L}$ and $\boldsymbol{S}$ denote the orbital and spin parts of the angular momentum operator, while $\boldsymbol{I}$ and $\boldsymbol{K}$ refer to the isospin and custodial SU(2) subgroups of SO(4).

The energy of the configurations is obtained by integrating the spherically symmetric energy density:

$$E = \frac{4\pi M_{\mathrm{W}}}{g^2} \int_0^\infty dx \Big(\frac{1}{2x^2}(f_A^2 + f_B^2 - 1)^2 + (f_A' + \frac{f_B f_C}{x})^2 + (f_B' - \frac{f_A f_C}{x})^2$$
$$+ (K^2 + H^2)(1 + f_A^2 + f_B^2 + \frac{f_C^2}{2}) + 2f_A(K^2 - H^2) - 4f_B HK$$
$$+ 2x^2(H'^2 + K'^2) - 2x f_C(K'H - KH') + \epsilon x^2 (H^2 + K^2 - 1)^2 \Big), \tag{2.9}$$

where we have introduced the dimensionless coordinate x

$$x = M_{\mathrm{W}} r, \tag{2.10a}$$

the prime denotes the derivative with respect to x, and the parameter ϵ related to the ratio, say R, of the boson masses (2.5)

$$\epsilon = \frac{4\lambda}{g^2} = \frac{1}{2}R^2, \qquad R \equiv \frac{M_{\mathrm{H}}}{M_{\mathrm{W}}}. \tag{2.10b}$$

The gauge invariance is not completely broken by the ansatz (2.6). Indeed, the U(1) gauge transformation

$$f_A + i f_B \to \exp(i\theta)(f_A + i f_B),$$
$$H + iK \to \exp\left(i\frac{\theta}{2}\right)(H + iK),$$
$$f_C \to f_C + x\theta', \tag{2.11}$$

leaves the energy density invariant for any radial function θ. To fix the gauge we choose

$$\text{(a)} \quad f_C(x) = 0, \qquad \text{(b)} \quad f_A(0) > 0, \qquad \text{(c)} \quad K(\infty) \leq 0. \tag{2.12}$$

The condition (a) corresponds to the radial gauge ($x_i V_i = 0$), it leaves a global U(1) ambiguity, which is fixed by (b) and (c) (from the first term in Eq. (2.9), it is obvious that f_A and f_B cannot vanish simultaneously at the origin). Still, the symmetries of the problem leave us with a degeneracy:

$$(f_A, f_B, H, K), \qquad (f_A, -f_B, -H, K). \tag{2.13}$$

i.e. a parity transformation (in fact supplemented by (2.11) with $\theta = 2\pi$, in order to restore (2.12(c))).

So far, two kinds of solutions of the classical field equations derived from the lagrangian (2.1) are known: the sphaleron and the deformed sphalerons. For reasons of completeness, we briefly recall their relevant features.

2.1. Sphaleron

Choosing the gauge (2.12), the sphaleron solution [4,5] has $f_B(x) = H(x) = 0$. The functions $f_A(x)$ and $K(x)$ are non-trivial and can be evaluated by numerical methods. The boundary conditions

$$\begin{aligned} f_A(0) &= 1, \qquad f_A(\infty) = -1, \\ K(0) &= 0, \qquad K(\infty) = -1, \end{aligned} \tag{2.14}$$

ensure that the solution is regular and that it has finite energy. The sphaleron can be constructed for all values of the mass ratio R. From (2.14) we see, that the length of the Higgs field vanishes at the origin; as a consequence, the solution becomes singular as $R \to \infty$, since in this limit, the Higgs field is frozen to its (non-vanishing) expectation value everywhere else.

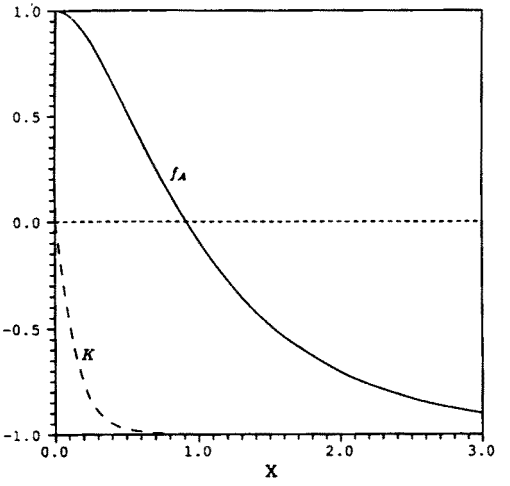

Fig. 1. The profiles of functions f_A and K of the sphaleron for $R = 13.5$.

The energy of the sphaleron increases monotonically with the mass ratio R from $E(R=0) \approx 7.06$ TeV to $E(R=\infty) \approx 12.57$ TeV for $M_W = 80$ GeV and $g = 0.65$. Further, the sphaleron is invariant under parity reflection (this is better seen after a rotation (2.11) with $\theta = \pi$). The radial functions of the sphaleron are presented in Fig. 1 for $R = 13.5$.

2.2. Deformed sphalerons

For sufficiently high values of the Higgs mass new extrema appear with an energy lower than the one of the sphaleron [6-8]. The new solutions, called deformed sphalerons, are not invariant under parity and appear as doublets of this operator. The boundary conditions for the radial functions read

$$\begin{aligned} f_A(0) &= 1, & f_A(\infty) &= \cos(\pi+\phi), \\ f_B(0) &= 0, & f_B(\infty) &= \sin(\pi+\phi), \\ H'(0) &= 0, & H(\infty) &= \cos\big((3\pi+\phi)/2\big), \\ K(0) &= 0, & K(\infty) &= \sin\big((3\pi+\phi)/2\big), \end{aligned} \tag{2.15}$$

where the angle ϕ depends on R.

The first deformed sphaleron appears for $R = R_1 \approx 12.04$. At the critical point, the deformed sphaleron coincides with the sphaleron. When R increases beyond R_1 the energy of the deformed sphaleron is lower than the energy of the sphaleron. The energy and the angle ϕ increase monotonically from $R = R_1$ to $R = \infty$. The numerical results for the first deformed sphaleron are

$$E(R_1) \approx 11.29 \text{ TeV}, \qquad E(\infty) \approx 11.78 \text{ TeV}, \tag{2.16}$$

$$\phi(R_1) = 0, \qquad \phi(\infty) \approx 0.403. \tag{2.17}$$

The radial functions of the first deformed sphaleron are presented in Fig. 2 for $R = 13.5$, *i.e.* slightly above the first critical value.

In Refs [6-8] it was shown that new branches of deformed sphalerons develop regularly when R increases. The second critical point is $R = R_2 \approx 138$. For this branch one finds

$$E(R_2) \approx 12.43 \text{ TeV}, \qquad E(\infty) \approx 12.50 \text{ TeV}, \tag{2.18}$$

$$\phi(R_2) = 0, \qquad \phi(\infty) \approx -0.121. \tag{2.19}$$

Finally, we want to stress that the deformed sphalerons converge to a smooth and regular limit as $R \to \infty$, providing a sequence of classical solutions with finite energy in the corresponding non-linear sigma model [7].

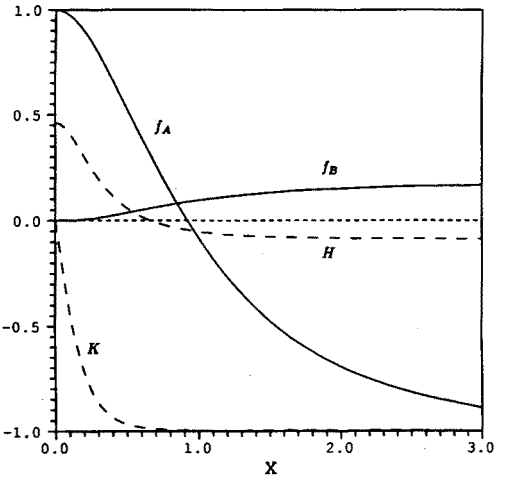

Fig. 2. The profiles of the functions f_A, f_B (solid lines) and H, K (dashed lines) for the deformed sphaleron for $R = 13.5$. the values of these functions at $x = 0$ (resp. $x = \infty$) are (1, 0, 0.46, 0) (resp.$\simeq$ (-0.98, 0.17, -0.08, -0.99)).

The radial functions of the first two elements of this sequence are presented in Figs 3 ($H^2 + K^2 = 1$ in this limit). The function K reaches its asymptotic value more rapidly, for each consecutive element of the sequence. Also we note, that the function H develops one more node for each consecutive element of the sequence.

3. Stability equations

To study the stability of a classical solution, the general way to proceed is to consider a general function, say $\psi(x,t)$ around it and to compute the Hamiltonian for this fluctuation; *i.e.* symbolically

$$H = H_{\mathbf{kin}} + H_{\mathbf{st}}, \tag{3.1}$$

$$H_{\mathbf{kin}} = \int d^3x\,(\dot{\psi})^2, \tag{3.2}$$

$$H_{\mathbf{st}} = E_{\mathbf{cl}} + \int d^3x\,(\psi M \psi) + O(\psi^3), \tag{3.3}$$

where $E_{\mathbf{cl}}$ denotes the classical energy and M the quadratic fluctuation matrix. This operator is hermitian, involves only spatial derivatives and depends on the classical fields. At first glance the diagonalisation of M appears to be very difficult, but the observation that it is invariant under

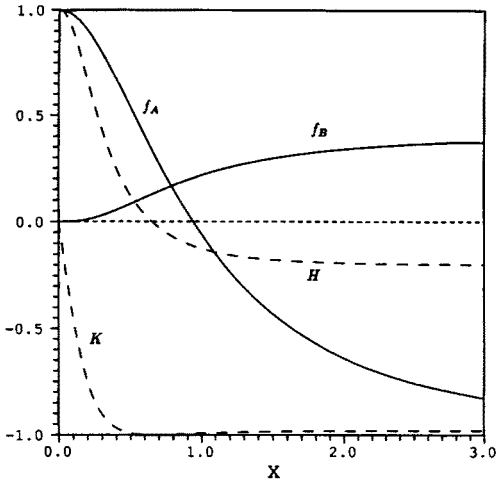

Fig. 3a. The profiles of the functions f_A, f_B (solid lines) and H, K (dashed lines) for the first deformed sphaleron for $R = \infty$. The values of the functions at $x = 0$ (resp. $x = \infty$) are (1, 0, 1, 0) (resp.$\simeq (-0.920, 0.392, -0.200, -0.979)$).

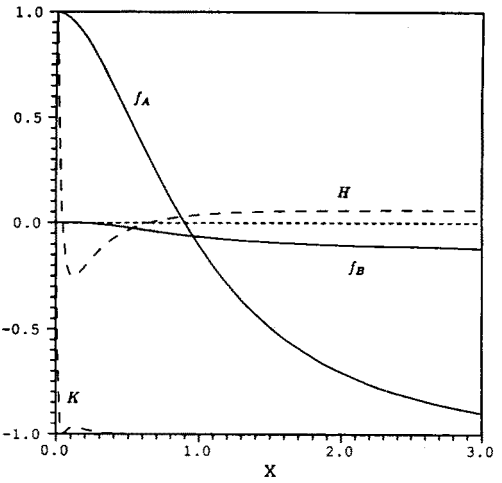

Fig. 3b. The profiles of the functions f_A f_B (solid lines) and H, K (dashed lines) for the second deformed sphaleron for $R = \infty$. The values at $x = 0$ (resp. $x = \infty$) are (1, 0, 1, 0) (resp. $\simeq (-0.992, -0.120, 0.060, -0.998)$).

the SU(2) group generated by J allows for an expansion of the fluctuation ψ in spherical harmonics of this operator. In this basis, the operator M decouples for the subspaces corresponding to the different harmonics.

Spherically symmetric fluctuations correspond to the lowest eigenvalue of J^2, *i.e.* $j = 0$. Here, we study the diagonalisation of the matrix M

restricted to this eigenspace; *i.e.* to the subspace of general spherically symmetric fluctuations, that we parameterize as follows:

$$\delta f_A = -\psi_A, \quad \delta f_B = \psi_B, \quad f_C = \sqrt{2}\psi_C, \quad \delta H = \frac{\psi_H}{\sqrt{2}x}, \quad \delta K = \frac{\psi_K}{\sqrt{2}x}. \tag{3.4}$$

The gauge symmetry is partly fixed by imposing $A_0 = 0$ also at the level of the fluctuations, the remaining gauge freedom is discussed below.

With this parametrization of the fluctuations, we expand the energy functional (2.9) up to second order in the fluctuations (3.4) $\psi_\alpha, (\alpha = A, B, C, H, K)$

$$E = E_{\rm cl} + \frac{4\pi M_{\rm W}}{g^2} \int (\psi^\dagger \Omega \psi)\, dx + \cdots \tag{3.5}$$

and focus on the quadratic term in ψ. After some algebraic manipulations, the relevant equations for the diagonalisation of the operator Ω can be written in the form

$$\begin{pmatrix} \psi_C' \\ \psi_A'' \\ \psi_B'' \\ \psi_H'' \\ \psi_K'' \end{pmatrix} = \begin{pmatrix} -(1/x) & \sqrt{2}(f_B/x) & \sqrt{2}(f_A/x) & -K & H \\ 2\sqrt{2}(f_B/x)' & V_{22} - \omega^2 & 0 & X & Y \\ 2\sqrt{2}(f_A/x)' & 0 & V_{33} - \omega^2 & Y & -X \\ -2K' & X & Y & V_{44} - \omega^2 & W \\ 2H' & Y & -X & W & V_{55} - \omega^2 \end{pmatrix} \times \begin{pmatrix} \psi_C \\ \psi_A \\ \psi_B \\ \psi_H \\ \psi_K \end{pmatrix}, \tag{3.6}$$

where ω^2 denotes an eigenvalue of Ω, and where we defined

$$\begin{aligned} V_{22} &= V_{33} = H^2 + K^2 + \frac{1}{x^2}(3f_A^2 + 3f_B^2 - 1), \\ V_{44} &= K^2 + \frac{(f_A - 1)^2 + f_B^2}{2x^2} + \frac{R^2}{2}(3H^2 + K^2 - 1), \\ V_{55} &= H^2 + \frac{(f_A + 1)^2 + f_B^2}{2x^2} + \frac{R^2}{2}(H^2 + 3K^2 - 1), \\ X &= -\frac{\sqrt{2}}{2}(H(1 - f_A) + K f_B), \\ Y &= \frac{\sqrt{2}}{2}(H f_B - K(f_A + 1)), \\ W &= (R^2 - 1)HK - \frac{f_B}{x^2}. \end{aligned} \tag{3.7}$$

Equation (3.6) resembles a system of coupled Schrödinger equations, but due to the equation for ψ_C it actually is not such a system. This first order equation is a consequence of the classical equations together with the eigenvalue equations of the operator Ω considered for a non-vanishing ω^2. It expresses the condition that the eigenvector ψ is orthogonal to all zero modes, existing due to the gauge symmetry.

We already noted that the sphaleron is invariant under parity. As a consequence of this discrete invariance, the equations for the (parity) even degrees of freedom decouple from the others, when Eq. (3.6) is considered in the background of a sphaleron. This is easy to see, since the off-diagonal potentials X and W vanish identically, when $H = f_B = 0$, so that the system (3.6) decouples into a system of three equations for ψ_C, ψ_B and ψ_H plus a system of two equations for ψ_A and ψ_H.

To form a normalizable eigenvector, the 5 functions ψ_α must satisfy the boundary conditions

$$\psi_\alpha(0) = \psi_\alpha(\infty) = 0, \qquad \alpha = A, B, C, H, K. \tag{3.8}$$

Using the asymptotic behaviour of the classical fields appearing in the potentials (3.7), one finds that the decay of $\psi_C(x)$ for large x follows a power law (first equation in (3.6)), while the other fluctuations decrease exponentially, provided

$$\begin{aligned} \omega^2 &< R^2 \qquad \text{if} \qquad R < 1, \\ \omega^2 &< 1 \qquad \text{if} \qquad R > 1, \end{aligned} \tag{3.9}$$

i.e. the lowest of the two masses M_{H} and M_{W} determines the boundary between the continuous and discrete parts of the spectrum.

4. Numerical results

We have studied Eq. (3.6) for the normal modes numerically in the background field of the sphaleron and the first few deformed sphalerons. The numerical results for the eigenvalues ω^2 are summarized in Table I, for various values of Higgs mass parameterized by the ratio R, covering the range $[0, \infty]$. The dependence of the eigenvalues on the ratio R is further shown in Fig. 4, where we represent the eigenvalues *via* the quantity

$$q = \mathrm{sign}(\omega^2) \cdot |\omega^2|^{1/4} \tag{4.1a}$$

and the mass ratio R *via*

$$p = \frac{1}{1 + \sqrt{\frac{R_1}{R}}}, \tag{4.1b}$$

TABLE I

Numerical estimations of the eigenvalues $-\omega^2$ for different values of the Higgs mass. The notations $a, b, \cdots, k$ refer to Fig. 4.

R	a	b	c	d	f	g	i	j	k
0.00	0.00	1.36							
0.50	−0.25	1.84							
1.00	−0.80	2.27							
1.50	−1.00	2.62							
2.00		2.93							
5.00		4.44							
9.00		6.75	−0.94						
10.00		7.42	−0.65						
12.00		9.30	−0.01						
12.04		9.38	0.00		9.38	0.00			
12.50		9.80	0.15		8.57	−0.27			
13.00		10.40	0.30		7.29	−0.50			
13.50		11.10	0.52		7.29	−0.74			
14.00		11.70	0.59		6.85	−1.00			
15.00		13.10	0.85		6.21				
20.00		22.50	1.87		4.96				
30.00		46.00	2.77		4.47				
50.00		147.00	4.04		4.10				
100.00		597.00	6.63		4.05				
112.00		752.00	7.44	−0.84	4.00				
120.00		865.00	8.07	−0.56	3.95				
138.20		1139.00	9.74	0.00	3.95		1139.0	9.74	0.0
140.00		1180.00	10.00	0.12	3.95		1093.0	9.48	−0.1
150.00		1357.00	11.20	0.35	3.95		859.0	7.92	−0.6
158.00		1507.00	12.20	0.67	3.95		725.0	6.98	−1.0
200.00		2360.00	19.00	1.66	3.95		401.0	5.56	
500.00		15000.00	127.00	3.95	3.95		205.0	4.41	
∞		∞	∞	∞	3.95		185.0	4.25	

so that the first critical point $R_1 = 12.04$ corresponds to $p = 0.5$. The solid lines labelled a, b, c, d represent the eigenvalues associated with the sphaleron, while the long (resp. short) dashed lines f, g (resp. i, j, k) correspond to the modes of the first (resp. second) deformed sphaleron.

In the background field of the sphaleron, the five equations (3.6) decouple into two systems of two (II channel) and of three (III channel) equations, respectively. The II channel admits a single normalisable eigenvector; for $R = 0$ this is a zero mode and it becomes a positive mode for $0 < R < 1.5$. For $R \approx 1.5$ the eigenvector disappears into the continuous part of the spectrum, as indicated in Fig. 4 by curve a.

For the III channel the situation is more complex and directly related

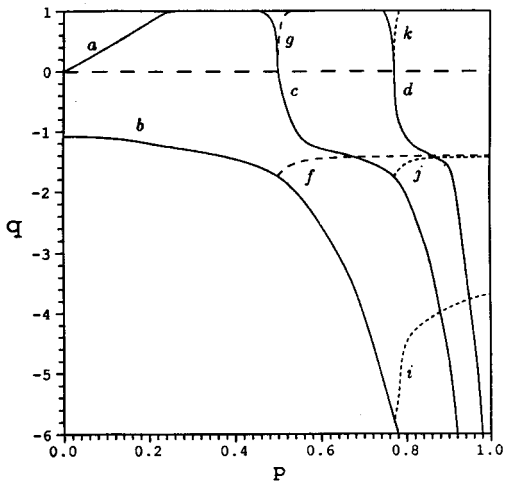

Fig. 4. The eigenvalues are plotted as functions of the Higgs mass *via* the quantities p, q defined in the text. The solid lines a, b, c, d refer to the eigenmodes about sphalerons. The long (resp. short) dashed lines f, g (resp. i, j, k) represent the eigenmodes about the first (resp. second) deformed sphaleron.

to the emergence of the deformed sphalerons. A negative eigenmode, represented by curve b in Fig. 4, exists for all values of R. This mode is the fundamental reason for the instability of the sphaleron, and it is the unique unstable mode up to $R = R_1$. For $R > R_1$ the sphaleron develops a second negative mode. The occurrence of this second mode is not spontaneous at $R = R_1$. Indeed, a second normalisable eigenvector emerges from the continuum for $R \approx 8.8$. Its eigenvalue (curve c in Fig. 4) decreases continuously from $\omega^2 = 1$ as R increases, it vanishes exactly at $R = R_1$ and then turns negative for $R > R_1$. The profiles of the two negative modes about the sphaleron are presented in Fig. 5 for $R = 13.5$. Note the power law decay of ψ_C in Fig. 5b.

The above scenario repeats in the neighbourhood of the second critical value ($R_2 \approx 138$). A third normalizable eigenvector of the III channel appears at $R \approx 110$ (curve d in Fig. 4) and crosses zero at R_2.

As R increases further the directions of instability increase in number and the lowest eigenvalues decrease strongly; this indicates that the sphaleron of Klinkhamer and Manton sits at the top of a very sharp energy barrier for very high values of the Higgs mass.

For $R > R_1$, the first deformed sphaleron appears as a new classical solution, approaching the profile of the sphaleron when $R \to R_1$. General considerations lead one to expect, that each discrete mode of the sphaleron, present at the bifurcation point, will also be present as a discrete mode

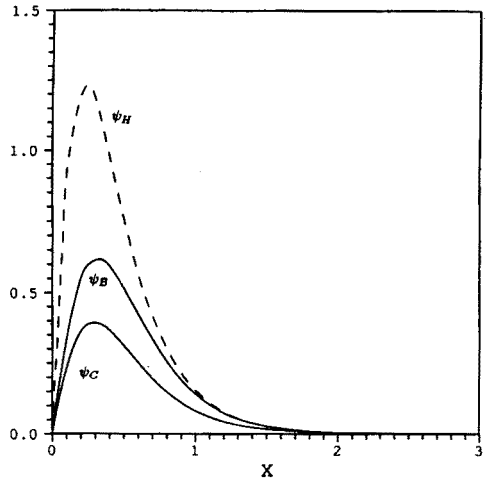

Fig. 5a. The profiles of the functions $\psi_i (i = B, C, H)$ of the first negative mode of the sphaleron for $R = 13.5$ $(\omega^2 = -11.1)$.

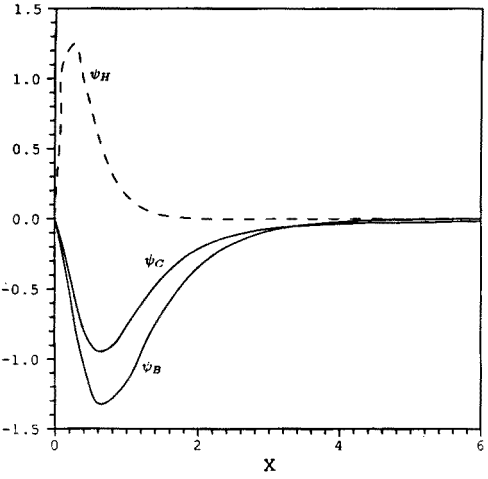

Fig. 5b. The profiles of the functions $\psi_i (i = B, C, H)$ of the second negative mode of the sphaleron for $R = 13.5$ $(\omega^2 = -0.52)$. The function ψ_H develops a node at $x \simeq 2.1$.

of the deformed sphaleron at the bifurcation point, since the two classical solutions merge at the critical point. Thus we expect two discrete modes of the first deformed sphaleron, one negative mode, starting from the negative mode of the sphaleron at the bifurcation point, and a second mode, starting from the zero mode of the sphaleron at the bifurcation point. Solving the full system (3.6) in the background field of the deformed sphaleron, we indeed

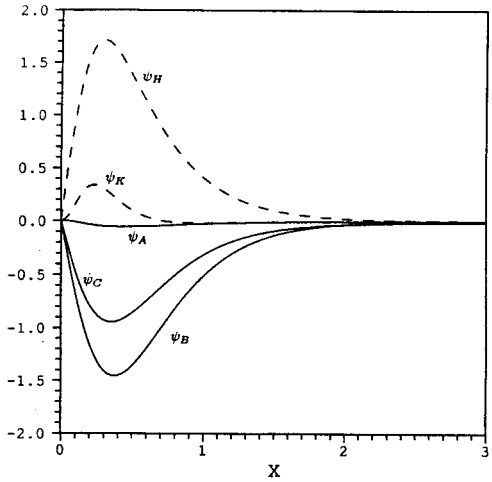

Fig. 6a. The profiles of the functions $\psi_i (i = A, B, C, H, K)$ for the negative mode of the deformed sphaleron for $R = 13.5$ ($\omega^2 = -7.29$). The function ψ_K develops a node at $x \simeq 0.70$.

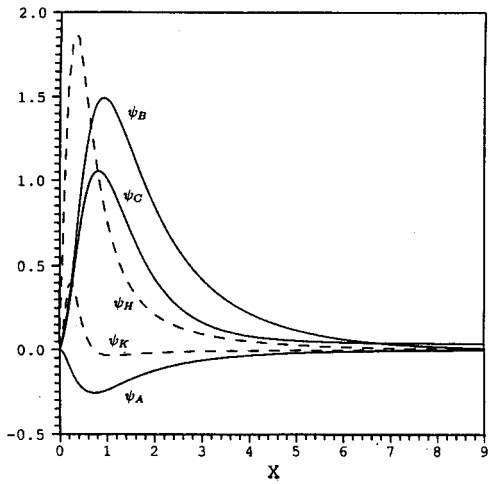

Fig. 6b. The profiles of the functions $\psi_i (i = A, B, C, H, K)$ for the positive mode of the deformed sphaleron for $R = 13.5$ ($\omega^2 = 0.74$). The function ψ_K develops a node at $x \simeq 0.72$.

find the expected negative mode, represented by curve f in Fig. 4. We also find a positive mode (curve g in Fig. 4), whose eigenvalue starts from zero at the bifurcation point, as expected, and merges into the continuum for $R \approx 15$. The profiles for the positive and the negative mode of the deformed sphaleron present at $R = 13.5$ are shown in Fig. 6. An important

point to stress is that the negative mode of the first deformed sphaleron persists and remains unique in the large R limit, $\omega^2 \to -3.95$ as $R \to \infty$.

The analysis of the system (3.6) in the background field of the second deformed sphaleron leads to an analogous scenario. Here, two negative modes appear (curves j, k in Fig. 4 along with a positive mode (curve i in Fig. 4). In the large R limit the two negative modes converge to $\omega^2 \approx -185.$ and $\omega^2 \approx -4.25$.

We note, that an analysis of the negative modes was reported previously [8], where, however, not the most general spherically symmetric fluctuations were considered (the excitation ψ_C was ignored). The results of [8] agree qualitatively with ours, though the numerical evaluations for the eigenvalues are considerably different. We further note, that our calculations for negative modes about the sphaleron agree with those of Refs [13-15], where only sphalerons were considered and the range of the Higgs mass was limited.

5. Conclusions

Non-abelian gauge theories are naturally associated with systems of non-linear equations, providing an impossible challenge to be solved completely. In the absence of techniques to obtain general solutions, one restricts the number of degrees of freedom by imposing symmetries on the solutions one is looking for. The larger is the symmetry, the simpler are the equations in principle.

In the case of the Weinberg–Salam model, no completely stable solution is expected to exist, apart from the vacua. However, unstable solutions can play a role in nonperturbative phenomena related to the multiple vacuum structure of the theory. For instance, sphalerons are the key ingredients in the computation of the rate of baryon number changing processes at finite temperature. Obviously, the non-trivial solution with the lowest energy should be relevant for such processes.

The "spherically symmetric" ansatz for the fields (2.6) corresponds to an SU(2)-like stability group, whose algebra is maximal among the set of transformations of the fields. For the sphaleron the stability group is even extended by the discrete group of parity transformations. For small values of the Higgs mass, where the sphaleron is the only known solution, it has a single unstable mode. When the first deformed sphaleron appears, it replaces the sphaleron as the lowest energy configuration. Then this first deformed sphaleron has an unique unstable direction, and in the large M_H limit its negative eigenvalue converges to a finite number. Yet, its stability group is SU(2), *i.e.* smaller than the one of the sphaleron. This raises the question about the possible existence of other solutions having lower energies and less symmetries.

The results of the analysis reported here agree with what Morse theory suggests about the geometry of the configuration space in the neighbourhood of the sphaleron [9]. Namely, if we denote C_q the number of critical points having q negative eigenvalues, the index χ defined as [18]

$$\chi = \sum_q (-1)^q C_q$$

is conserved for all values of the Higgs mass, provided the sum is taken over all known critical points: sphalerons and pairs of deformed sphalerons. Interestingly, the situation encountered in the Weinberg–Salam model (for $\theta_W = 0$) is very similar to the case of a $1 + 1$ dimensional field theory, investigated by Manton and Samols [19].

REFERENCES

[1] G.'t Hooft, *Phys. Rev. Lett.* **37**, 8 (1976).
[2] V. Kuzmin, V. Rubakov, M. Shaposhnikov, *Phys. Lett.* **155B**, 36 (1985).
[3] N. Manton, *Phys. Rev.* **D28**, 2019 (1983).
[4] F. Klinkhamer, N. Manton, *Phys. Rev.* **D30**, 2212 (1984).
[5] R. Dashen, B. Hasslacher, A. Neveu, *Phys. Rev.* **D10**, 4138 (1974).
[6] J. Kunz, Y. Brihaye, *Phys. Lett.* **216B**, 353 (1989).
[7] Y. Brihaye, J. Kunz, *Mod. Phys. Lett.* **A4**, 2723 (1989).
[8] L.G. Yaffe, *Phys. Rev.* **D40**, 3463 (1989).
[9] F. Klinkhamer, *Phys. Lett.* **B236**, 187 (1990).
[10] J. Langer, *Ann. Phys. (N.Y.)* **41**, 108 (1967); **54**, 258 (1969).
[11] I. Affleck, *Phys. Rev. Lett.* **46**, 388 (1981).
[12] P. Arnold, L. McLerran, *Phys. Rev.* **D36**, 581 (1987); **D37**, 1020 (1988).
[13] T. Akiba, H. Kikuchi, T. Yanagida, *Phys. Rev.* **D40**, 588 (1989).
[14] L.Carson, L. McLerran, *Phys. Rev.* **D41**, 647 (1990).
[15] L. Carson, Xu Li, L. McLerran, R.-T. Wang, *Phys. Rev.* **D42**, 2127 (1990).
[16] Y. Brihaye, S. Giler, P. Kosinski, J. Kunz, *Phys. Rev.* **D42**, 2846 (1990).
[17] Y. Brihaye, J. Kunz, *Phys. Lett.* **B249**, 90 (1990).
[18] J. Milnor, *Morse Theory, Ann. of Math. Studies* No 51, Princeton U.P., 1973.
[19] N.S. Manton, T.M. Samols, *Phys. Lett.* **B207**, 179 (1988).